Impact of seismic tomography on earth sciences

Dapeng Zhao*,† and J. R. Kayal‡

†Department of Earth Sciences, Ehime University, Matsuyama 790, Japan
‡Geological Survey of India, 4 Chowringhee Lane, Calcutta 700 016, India

Seismic tomography signifies a revolution in earth sciences. It has had far-reaching and deep impacts on the geological community and it will continue to influence the future developments in earth sciences. In this article, we have reviewed the recent results of tomographic studies, including the advances in tomographic methodology. Tomographic imaging has been particularly successful in understanding the mechanism of subducting slab and arc magmatism, structure and process in the source zones of large earthquakes and the earth's deep structure and dynamics.

Introduction

During the 20th century, seismologists had made a number of important discoveries that had far-reaching and profound impacts on earth sciences, such as the establishment of layered structure of the earth's interior and the discovery of deep-focus earthquakes[1]. Seismic tomography is the latest tool that seismologists have provided the geological community and it has greatly influenced the developments in earth sciences. With its vast scope in understanding the earth's structure and processes, its influence will continue for several decades to come. In this article we review the recent developments in seismic tomography, including its methodology and applications.

Once an earthquake occurs, it generates seismic waves that pass through the earth's interior and finally arrive at the earth's surface, where they are recorded by seismographs. Analyses of the observed seismic waves provide information on the rupture process of the earthquake as well as physical properties of the materials along the wave trajectories. The classic studies of seismic waves have led to the discoveries of the layered structure of the earth. Since the advent of seismic tomography two decades ago[2], seismologists have been mapping the heterogeneous structure of the earth on a broad range of scales. These three-dimensional (3D) models of the earth's structure promise to answer some basic questions of geodynamics and signify a revolution in earth science[3]. At present, seismic tomography is developing at an accelerated pace and it is expected to be an active field of seismological research for several decades to come[4].

During the last two decades, thanks to the advances in seismic tomography techniques and the installation of dense regional and global seismographic networks, seismologists have made significant progress in understanding the structure, magmatism and dynamics of the earth. In this article some of the recent observations borne out of tomographic studies are discussed. Numerous such studies have been published in the literature, and it would be impossible to do a thorough review on all of them in this limited space. Therefore, here we will mainly introduce the studies that we are involved in or are familiar with. Before describing the major impacts of seismic tomography on earth sciences, let us first do a brief review of the recent advances in the methodology of seismic tomography.

Advances in seismic tomography methodology

Most of the early studies used the first tomographic method[2] that divides the medium under study into many cubic blocks and treats seismic velocities in every block as unknown parameters. Unavoidably, this first method has several drawbacks. For example, artificial velocity discontinuities are introduced into the model between blocks; seismic rays are assumed to be beelines within each block; and only one iteration of inversion is conducted. Grid nodes, instead of blocks, were later adopted to model the earth structure[5]. In the later model, velocities at the nodes are treated as unknown parameters but their value at any point in the model is calculated by interpolating velocities at eight nodes surrounding that point. Thus, this model treats velocity as continuous everywhere in the model and no velocity discontinuity is allowed to exist even when discontinuities are actually detected in the study area. In addition, Thurber[5] adopted Cartesian coordinates, hence his method has been applied mainly to local-scale studies.

Japan provides an ideal location for the illustration of some of the inherent weaknesses of these earlier methods. Japan is located in a complex region where the Pacific, Eurasian, North American and Philippine Sea plates are interacting with each other. The upper boundary of the subducted Pacific slab is a sharp seismic discontinuity with a complex geometry[6,7]. The Moho and the Conrad discontinuities also have large depth variations[8]. These discontinuities generate clear converted and reflected seismic waves observable in seismograms[6–8] and should be taken into account when studying the 3D earth struc-

*For correspondence. (e-mail: zhao@sci.ehime-u.ac.jp)

ture. In principle, when the block or grid size is sufficiently small, the effects of the discontinuities can be evaluated. The size in actual studies, however, is not small enough because of the sparse distribution of seismic stations. Hence the tomographic images obtained not only represent velocity variations themselves, but also contain the effects of discontinuity undulations[9]. Without introducing discontinuities into the model, the converted and reflected phase data cannot be used. These phases that are late arrivals contain important information about the earth structure that can be used for improving the ray path coverage and the accuracy of earthquake locations. However, neither Aki nor Thurber's methods[2,5] can handle the complex discontinuities and the later phase data.

To tackle these problems, an improved tomography method was developed[9]. The medium under study is divided into layers bounded by the discontinuities that have been known to exist. 3D grid nets are set individually in each of the layers. A new 3D ray tracing technique is developed to compute travel times and ray paths in such a model[9]. First P and S waves and later phase data can all be used in the tomographic inversion. A conjugate-gradient algorithm is used to conduct inversion so that a great number of data can be used to determine a detailed 3D structure. This method was further improved to make it use data from local, regional and teleseismic events simultaneously[10,11]. Recently, this method was extended to the global scale to estimate the whole mantle 3D structure[12]. Other recent developments include combining teleseismic polarization data with arrival times[13], formulating the problem of travel-time inversion for both velocity heterogeneity and anisotropy[14] and using teleseismic P-wave amplitudes together with travel times[15].

Subducting slab and arc magmatism

Zhao and his coworkers[9,10] applied their new tomography method to over 50,000 arrival times from local, regional and teleseismic events to determine a detailed 3D P-wave velocity structure of the Japan subduction zone. In addition to first P and S wave data, they also used converted waves at the subducting slab boundary and the Moho discontinuity. Figure 1 shows the P-wave tomography in north-east Japan which they obtained. The spatial resolution of the image is 25 to 30 km in a horizontal direction and 10 to 25 km in depth. The subducting cold Pacific slab is clearly imaged with a thickness of 90 km and a P-wave velocity 4 to 6% higher than the normal mantle. Intermediate-depth earthquakes occur in the subducting slab and form two distinct seismic planes, the so-called double seismic zone[6]. Low velocity (low-V) zones are visible just beneath the active volcanoes, and extend to 150 km depth in the mantle wedge. Anomalously low-frequency microearthquakes occur around the low-V zones beneath active volcanoes in the depth range of 25 to

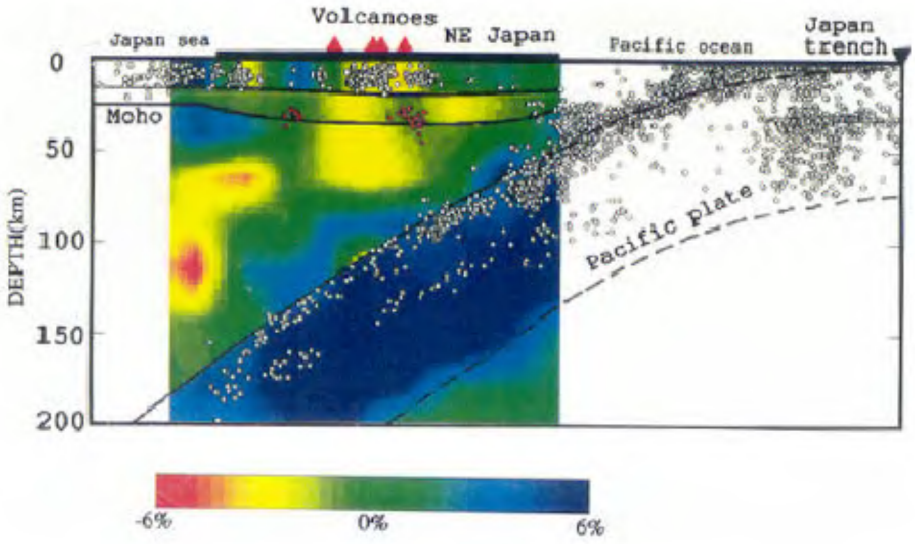

Figure 1. Vertical cross-section of P-wave velocity structure beneath north-east Japan from the earth's surface to 200 km depth along 40 degrees north latitude. Red and blue colours denote slow and fast velocities, respectively. The velocity perturbation scale is shown at the bottom. Open circles denote earthquakes that occurred within a 40-km width along the profile. Red circles show low-frequency microearthquakes that occurred around the Moho discontinuity, due to the magmatic and volcanic activity. Red triangles represent active volcanoes and the black reverse triangle shows the location of the Japan trench. The thick horizontal line at the top of the cross-section shows the land area where seismic stations exist. The three thick curved lines denote the Conrad and Moho discontinuities and the upper boundary of the subducting Pacific slab. The dashed line shows the lower boundary of the slab. Shallow earthquakes occur in the upper crust; intermediate-depth and deep earthquakes occur in the subducting slab.

47 km, which were caused by the magmatic and volcanic activity[16]. Distinct shear-wave reflectors are also found near the low-V zones in the lower crust, which represent the upper surface of hot magma chambers with a thickness of about 100 m (ref. 16). The low-V zones in the crust and mantle wedge also exhibit strong seismic attenuation (low-Q) (ref. 17). Based on these observations, we believe that these low-V/low-Q zones are associated with the magma chambers, which form the roots of the arc volcanoes.

Mineral physics studies have revealed detailed behaviours of phase changes of some mantle minerals such as olivine, wadsleyite and ringwoodite at high temperature and high pressure conditions. It is believed that the dehydration of the subducted oceanic crust and convective circulations in the mantle wedge may have played an important role in the generation of melts and magma in the mantle wedge of island arcs[18–20]. The low-V/low-Q zones in Figure 1 may represent these processes.

Figure 1 shows some heterogeneities within the subducting Pacific slab. It is found from plane map views that earthquakes within the slab (the lower-plane events in the double seismic zone) occur in relatively higher velocity areas of the slab[9]. There may be two reasons for the origin of heterogeneity in the slab. One is the assumption that heterogeneity originally associated with seamounts, ridges and fracture zones[7] existed in the oceanic plate before subduction, as can be seen clearly from the bathymetric map of oceanic floors. The other is related to the complex phase changes of the rocks within the slab, caused by the increasing temperature and pressure during the subduction of the oceanic plate[21].

Deep dehydration and back-arc spreading

Most of the seismic stations in Japan are located on the narrow islands of about 200 km wide, hence high-resolution tomographic images are determined only down to about 200 km depth (Figure 1). The depth extent of the low-V zones in the mantle wedge is not clear in the back-arc region. Recently, data recorded by land seismic stations and ocean bottom seismographs (OBS) were used to determine a detailed 3D structure down to 700 km depth beneath the Tonga arc and the Lau back-arc[11] (Figure 2). The subducting Tonga slab is imaged as a 100-km-thick zone with a *P*-wave velocity 4 to 6% higher than the surrounding mantle. Beneath the Tonga arc and the Lau back-arc, low-V anomalies of up to 6% are visible. The low-V anomaly beneath the Tonga arc represents a dipping zone about 30 to 50 km above the slab, extending from the surface to about 140 km depth. This feature is similar to the low-V zones found beneath the Japan volcanic front (Figure 1). Beneath 100 km, the amplitude of the back-arc anomalies is reduced, but a moderately slow anomaly (– 2 to – 4%) exists down to a depth of at least 400 km. Extent of the mantle wedge slow anomalies to these depths has been confirmed by detailed resolution analyses[11], attenuation tomography[22], and waveform modelling[11,23]. These results indicate that geodynamic systems associated with the back-arc spreading are not limited to the near-surface areas, but are related to deep processes.

The slow velocity anomalies at depths of 300 to 400 km in the mantle wedge (Figure 2) could be caused by upwelling flow patterns in the mantle wedge or by volatiles resulting from the deep dehydration reactions occurring in the subducting slab. Volatiles would have the effect of lowering the melting temperature and the seismic velocity, and may produce small amounts of partial melt. Temperatures in fast subducting slabs like Tonga are low enough for water to reach the stability depths of dense hydrous magnesium silicate phases[24], which may allow water penetration down to depths of 660 km. The phase diagrams of important hydrous phases, the associated reaction kinetics, and the relevant mantle conditions (slab temperature and composition) are not known sufficiently well to predict the depth at which dehydration would occur. Partial melting of the mantle wedge by volatiles from the deep slab may be important in localizing low seismic velocities; the slow anomalies we observe at depths of 300 to 400 km (Figure 2) may represent this process.

The slow velocity regions beneath the Tonga arc and the Lau back-arc seem to be separated at the shallow levels, but merge at depths greater than 100 km (Figure 2). This suggests that although the arc and back-arc magma systems are separated at shallow levels, where most of the magma is generated, there may be some interchange between the magma systems at depths greater than

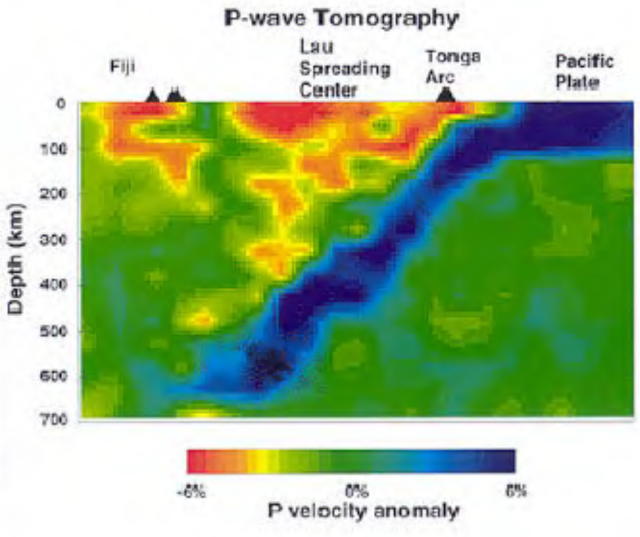

Figure 2. East-west, vertical cross-section of *P*-wave velocity image from 0 to 700 km depth beneath the Tonga arc and Lau back-arc region. Red and blue colours denote slow and fast velocities, respectively. Solid triangles denote active volcanoes. Earthquakes within a 40-km width from the cross-section are shown in open circles. The velocity perturbation scale is shown at the bottom.

100 km. Interchange with slab-derived volatiles at depths greater than 100 km may help to explain some of the unique features in the petrology of back-arc magmas relative to typical mid-ocean ridge basalts, including excess volatiles and large ion lithophile enrichment[25].

Influence of magmas on large crustal earthquakes

Many countries have suffered heavily and frequently from earthquake hazards. A good understanding of where large crustal earthquakes occur is important for the clarification of physics of earthquake generation and for the mitigation of seismic hazards. Zhao *et al.*[26] investigated the relationship between the 3D crustal structure and the distribution of large crustal earthquakes in Japan in the recent history. They found that most of the 160 large crustal earthquakes (magnitude 5.7 to 8.0; depth 0 to 20 km) during a period of 115 years from 1885 to 1999 occurred around zones of low seismic velocity revealed by seismic tomography (Figure 3). The low-V zones may represent weak sections of the seismogenic crust. Crustal weakening along the volcanic front and in back-arc areas may be caused by active volcanoes and magma chambers. Low-V zones in the uppermost mantle may be the manifestation of mantle diapirs associated with the ascending flow of subduction-induced convection in the mantle wedge and dehydration reactions in the subducting slab[9] (Figure 1). Magmas further rising from the mantle diapirs to the crust may cause low-frequency microearthquakes at levels of the lower crust and uppermost mantle, and make their appearance as *S*-wave reflectors at midcrustal levels. Their upward intrusion raises the temperature and reduces the seismic velocity of crustal materials around them, causing the overlying brittle seismogenic layer to become locally thinner and weaker. This can be seen clearly from the distribution of crustal seismicity in volcanic areas[26]. The cut-off depth of the crustal earthquakes is elevated toward the volcanoes, indicating a higher temperature and a thinner brittle seismogenic layer beneath the active volcanoes[26].

Subject to the horizontal compressional stress field in the plate convergence direction, contractive deformations will take place mainly in the low-V, low-Q areas because of the thinner and brittle seismogenic layer, weaker crust and uppermost mantle, due to the higher temperature. Deformation occurs partially as small earthquakes but mainly as plastic deformation, causing the crustal shortening, upheaval and mountain building. Large crustal earthquakes cannot occur within the weak low-V zones but in their edges, where the mechanical strength of materials is higher compared to the low-V zones, but still weaker than the normal sections of the seismogenic layer. Thus, the edge portion of the low-V areas becomes the ideal locations to generate large earthquakes (Figure 4).

Fluids at the heart of large earthquakes

The 17 January 1995 Kobe earthquake (*M* 7.2) occurred in the upper crust in south-west Japan, and caused over 6400 fatalities and tremendous property losses. Detailed 3D, *P* and *S* wave velocity and Poisson's ratio structures were determined in the Kobe fault zone with a spatial

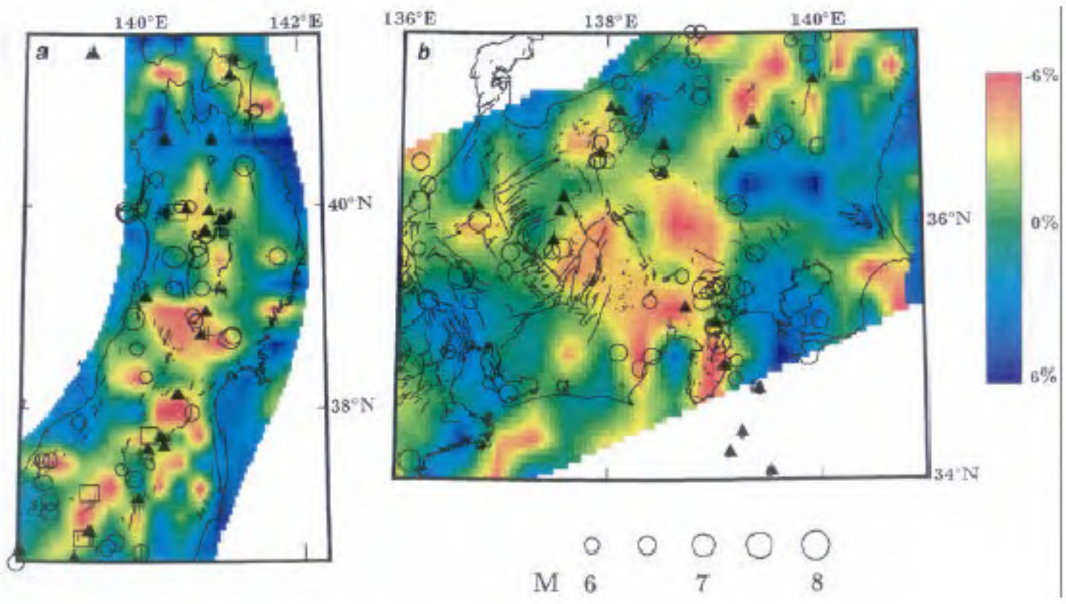

Figure 3. *P*-wave velocity image at a depth of 40 km beneath (***a***) north-east and (***b***) central Japan. Red and blue colours denote low and high velocities, respectively. Circles denote earthquakes (*M* 5.7–8.0, depth 0–20 km) that occurred during a period of 115 years from 1885 through 1999. Solid triangles denote active volcanoes. Active faults are shown by thick lines. The velocity perturbation scale and the earthquake magnitude scale are shown on the right and at the bottom, respectively. Crosses and open squares in (***a***) show low-frequency microearthquakes and *S*-wave reflectors in the mid-crust, respectively.

resolution of 4–5 km (Figure 5)[27,28]. The hypocentre of the Kobe main shock is located in a distinctive zone characterized by low P and S wave velocities and high Poisson's ratio. This anomaly exists in the depth range of 16 to 21 km, and extends 15 to 20 km laterally, which is interpreted to be a fluid-filled, fractured rock matrix that contributed to the initiation of the Kobe earthquake. This interpretation has been supported by many evidences from hydrological, geochemical, seismological and geophysical investigations conducted in the Kobe earthquake region[28].

There are two possibilities of the origin of fluids in the Kobe fault zone. One, the shallow source such as fluids trapped in the pore spaces, those originating from mineral dehydration in the crust, and through the permeation of the meteoric and sea waters down to the deep crust through the active faults that would have been ruptured during many earthquake cycles[29]. The other is of deep origins such as the dehydration of the subducting Philippine Sea slab.

To unravel the structure of the subducting Philippine Sea slab and its effect on the Kobe earthquake, the 3D velocity structure of the crust and upper mantle under south-west Japan was investigated in detail (Figure 6)[26]. The subducting Philippine Sea slab is imaged clearly. It has a thickness of 30–35 km and a P-velocity 3 to 5% higher than that of the normal mantle. A prominent low-V zone exists in the lower crust (16–30 km depth) and right above the subducted Philippine Sea slab. This low-V zone has properties as the anomaly at the Kobe hypocentre which shows low Vp, low Vs and high Poisson's ratio[27,28]. These results suggest that the fluids that contributed to the initiation of the 1995 Kobe earthquake may be related to the dehydration process of the subducted Philippine Sea slab. This argues for a deeper source, but it is also possible that the fluids are of shallow origin through processes mentioned earlier. It is generally considered that fluids widely exist in the crust and uppermost mantle in the fore-arc regions of subduction zones[19,20]. The Philippine Sea plate is descending at a very small dip angle in Shikoku and eastern Kii Peninsula, and the subducting slab is located right under the crust[30]; thus the fluids from the slab dehydration may easily migrate upwards to the crust. Migration of fluids to the active faults in the crust (such as the Nojima Fault that generated the 1995 Kobe earthquake), will lead to increase in pore pressures with a decrease in the effective strength of the fault. Through these processes, active faults can be weakened to generate large crustal earthquakes.

The evidences discussed here (Figures 3–6) suggest that the generation of a large crustal earthquake is closely related to the surrounding tectonic environment such as plate subduction and physical/chemical properties of crustal materials, such as magmas, fluids, etc. The rupture nucleation zone should have a three-dimensional spatial extent, not just limited to the two-dimensional surface of a fault, as suggested earlier in the concept of earthquake volume[31]. Complex physical and chemical reactions may take place in the source zones of future earthquakes, causing heterogeneities in the material property and stress field, which may be detected with seismic tomography and other geophysical methods. The source zone of a M 6 to 8 earthquake extends from about 10 km to over 100 km (ref. 32). The resolution of our tomographic imaging is close to that scale of the earthquake sources, which may have enabled us to image the earthquake-related heterogeneities in the crust and uppermost mantle in Japan.

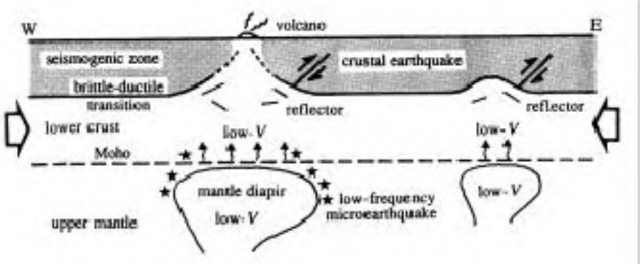

Figure 4. Schematic illustration of across-arc vertical cross-section of the crust and uppermost mantle in volcanic areas of Japan, showing the cause of large crustal earthquakes and their relation to low-velocity zones and magma chambers in the uppermost mantle.

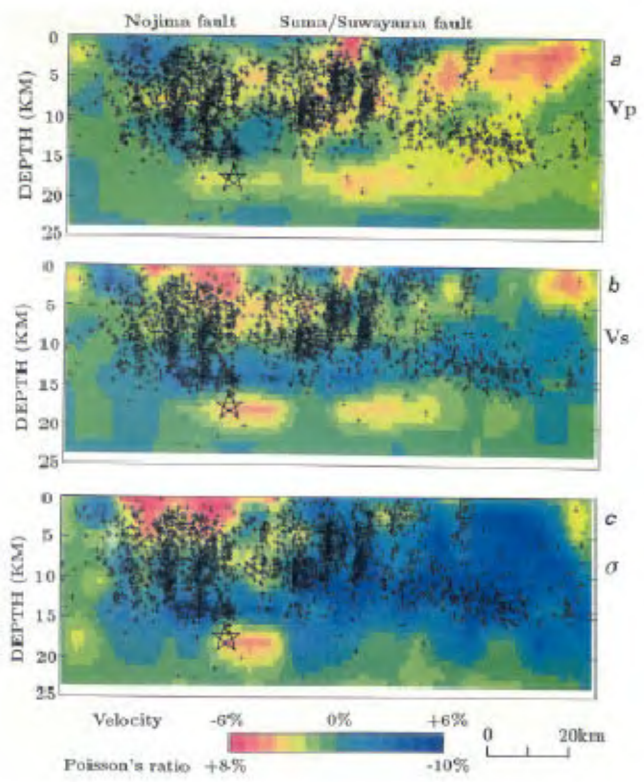

Figure 5. Vertical cross-sections of (***a***) P-wave velocity (V_p), (***b***) S-wave velocity (V_s), and (***c***) Poisson's ratio along the Kobe fault zone. Slow velocity and high Poisson's ratio are shown in red; fast velocity and low Poisson's ratio are shown in blue. V_p and V_s perturbations range from – 6% to 6% from the 1D velocity model. Poisson's ratio ranges from 0.225 to 0.27 (– 10% to 8% from the average value). Small crosses denote the Kobe aftershocks within a 6-km width along the Kobe fault zone. The star denotes the hypocenter of the Kobe mainshock; its focal depth is 17.7 km. The vertical exaggeration is 2 : 1.

These results indicate that large earthquakes do not strike just anywhere, but only in anomalous areas that may be detected with geophysical methods. This has important implications for the understanding of earthquake-generating processes and identification of potential source zones, leading to effective hazard mitigation.

Deep earth structure and dynamics

Figure 7 shows a 3D image of *P*-wave velocity structure down to the core–mantle boundary under the Pacific Ocean[12]. Compared with the previous whole mantle tomography models[33,34], this new model has the following features. It adopted a grid parameterization[9] instead of blocks, which are used in most of the global travel-time tomographic studies. Ray paths and travel times are computed with an efficient 3D ray tracing scheme[9]. Another unique feature of the new model is that recent results[35] on the topography of mantle discontinuities are taken into account in the tomographic inversion. The 410- and 660-km discontinuities have large lateral depth variations of up to 36 km (ref. 35). It is found that there are considerable changes in the tomographic images in and around the transition zone when the discontinuity topography is taken into account, particularly for high-resolution models with smaller grids. In general, final travel time residuals become smaller for the tomographic models including the discontinuity topography, indicating that it is necessary to take into account the discontinuity topography in order to image the detailed structure of the mantle transition zone.

A large amount of International Seismological Centre (ISC) travel times (P, PP, PcP, pP) were used to derive the new model of whole mantle tomography[12]. This new model contains the general features observed in the previous models: a low-velocity ring around the Pacific Ocean basin in the depth range of 0–400 km, and high-velocity anomalies surrounding the Pacific basin just above the core-mantle boundary. One significant difference from the previous models is that much stronger and wider high-velocity anomalies are visible in the transition zone depths under the subduction zones. This is an indication that most of the slab materials are stagnant for a long time in the transition zone before finally dropping down to the lower mantle, and some of the slabs may only stay above the 670 km discontinuity and complete their convections within the upper mantle. Plume-like slow anomalies are visible under the hot spot regions with different depth extensions, suggesting that not all hot spots and plumes originate at the core–mantle boundary; some of them may originate at lower to middle mantle depths. These results may improve our understanding of the structure and dynamics of the earth's deep interior.

Concluding remarks

Although great advances have been made in seismic tomography and its applications in the last two decades, a great deal remains to be done in future in both theoretical

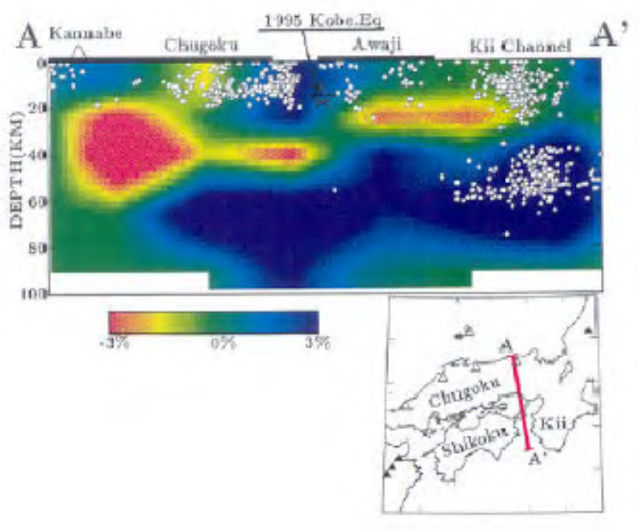

Figure 6. Vertical cross-section of *P*-wave velocity structure down to a depth of 100 km along the line AA′ in the insert map. Blue and red colours denote fast and slow velocities, respectively. The velocity perturbation scale is shown at the bottom. The star symbol shows the hypocenter of the 1995 Kobe mainshock (*M* 7.2). White dots show the microearthquakes within a 20-km width from the line AA′, which occurred during 1985 to 1993. The thick lines on the top show the land areas, the Chugoku District and Awaji Island. The open triangle denotes the Kannabe Quaternary volcano in Chugoku.

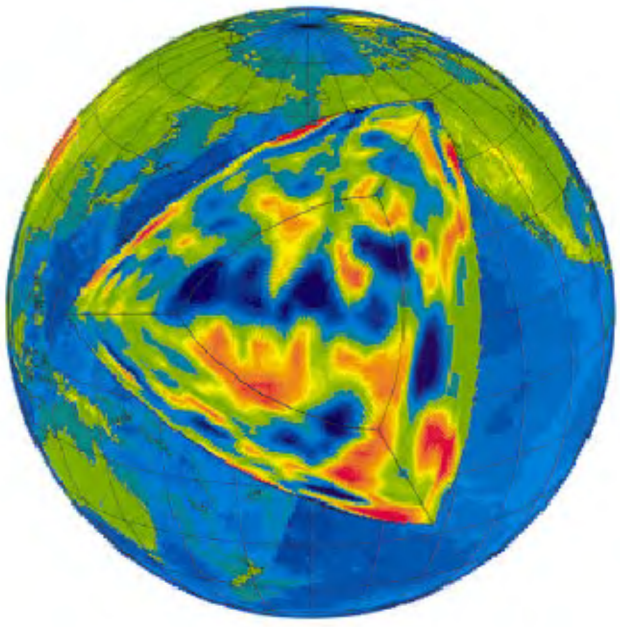

Figure 7. Three-dimensional image of *P*-wave velocity structure down to the core–mantle boundary under the Pacific Ocean. The image within the central triangle shows velocity variations on the core–mantle boundary. The surrounding three fans show the velocity images of the whole mantle along each cross-section. The remaining parts show the earth's surface topography. Blue and red colours denote fast and slow velocities, respectively. The velocity perturbations are from – 1% to + 1%, deviating from the one-dimensional earth model.

development and in imaging of the earth structure. The existing schemes of model parameterization need to be thoroughly compared and examined; new and more adequate parameterization of the earth structure should be explored continuously. The effort to search better 3D ray tracing and inversion algorithms should be continued. Large data sets of converted and reflected waves should be collected to improve the spatial resolution of tomographic models in both local/regional and global scales. Amplitudes, polarizations and waveforms should be used together with arrival times to obtain better 3D seismic velocity and attenuation models. Anisotropy tomography methods should be better studied by jointly using arrival times, differential times of splitting shear waves and surface wave dispersion data.

More work remains to be done on the application of tomography methods to the imaging of the earth structure, which largely depends on the installation of new permanent or portable seismic networks or the enlargement of the existing networks. Most of the current seismic stations are located on continents and islands, installing of OBS seismic networks on the broad ocean bottoms will be crucial for future seismological researches.

Although seismic tomographers have revealed significant lateral heterogeneities in the crust and mantle on various scales, many branches of seismology (such as the studies of earthquake source mechanisms and waveform modelling) are still using simple, one-dimensional models. The old geophysical picture of a simple layered earth model should be abandoned[5]. All the future seismological studies should be based on the 3D earth models.

So far, most of the studies on earthquake sources have concentrated on the coseismic rupture process on the fault plane by analysing the seismic waves generated during the faulting, which provides little information on the preparatory process of the earthquakes. This gap would be filled with high-resolution tomographic imagings of the earthquake source areas and active fault zones. The effects of inelastic structures, presence of magmas and fluids in the crust and upper mantle on the generation of earthquakes deserve special attention.

The limitations of seismic tomography have also become apparent. The tomograms simply represent kinetic snapshots of the earth, and do not directly show the earth's dynamic processes. This may be improved by incorporating seismic anisotropy in tomographic inversions, as has been done in some studies with surface waves. Similarly, tomograms show only the earth's current images (strictly speaking, the images during the period when the data are collected), which represent the summation of all the changes that happened during the past geological history. Future studies may try to detect temporal variations of some of the geological phenomena, such as the images before, during and after the eruption of active volcanoes and the occurrence of large earthquakes, which would be useful for the hazard assessment and mitigation.

The challenge is great, but with ingenuity, striving and cooperation we can anticipate exciting new advances in seismic tomography and the understanding of the earth structure and dynamics in the twenty-first century.

1. Aki, K., *Geol. Soc. Am. Bull.*, 1988, **100**, 625–629.
2. Aki, K. and Lee, W., *J. Geophys. Res.*, 1976, **81**, 4381–4399.
3. Dziewonski, A. and Anderson, D., *Am. Sci.*, 1984, **72**, 483–494.
4. Iyer, H., in *The Encyclopedia of Solid Earth Geophysics* (ed. James, D.), Van Nostrand Reinhold, New York, 1989, pp. 1133–1151.
5. Thurber, C., *J. Geophys. Res.*, 1983, **88**, 8226–8236.
6. Hasegawa, A., Umino, N. and Takagi, A., *Geophys. J. R. Astron. Soc.*, 1978, **54**, 281–296.
7. Zhao, D., Matsuzawa, T. and Hasegawa, A., *Phys. Earth Planet. Inter.*, 1997, **102**, 89–104.
8. Zhao, D., Horiuchi, S. and Hasegawa, A., *Tectonophysics*, 1992, **212**, 289–301.
9. Zhao, D., Hasegawa, A. and Horiuchi, S., *J. Geophys. Res.*, 1992, **97**, 19909–19928.
10. Zhao, D., Hasegawa, A. and Kanamori, H., *J. Geophys. Res.*, 1994, **99**, 22313–22329.
11. Zhao, D., Xu, Y., Wiens, D., Dorman, L., Hildebrand, J. and Webb, S., *Science*, 1997, **278**, 254–257.
12. Zhao, D., *Eos Trans. AGU*, 1999, **80**, 716.
13. Hu, G., Menke, W. and Powell, C., *J. Geophys. Res.*, 1994, **99**, 15245–15256.
14. Wu, H. and Lees, J., *Geophys. J. Int.*, 1999, **137**, 64–80.
15. Neele, F., VanDecar, J. and Snieder, R., *J. Geophys. Res.*, 1993, **98**, 12033–12054.
16. Hasegawa, A. and Zhao, D., in *Magmatic Systems* (ed. Ryan, M. P.), Academic Press, San Diego, 1994, pp. 179–195.
17. Tsumura, N., Hasegawa, A. and Horiuchi, S., *Phys. Earth Planet. Inter.*, 1996, **93**, 105–121.
18. Ringwood, A., *J. Geol.*, 1982, **90**, 611–643.
19. Tatsumi, Y., *J. Geophys. Res.*, 1989, **94**, 4697–4707.
20. Iwamori, H. and Zhao, D., *Geophys. Res. Lett.*, 2000, **27**, 425–428.
21. Kao, H. and Liu, L., *Geophys. J. Int.*, 1995, **123**, 71–84.
22. Roth, E., Wiens, D. and Zhao, D., *Geophys. Res. Lett.*, 2000, **27**, 601–604.
23. Xu, Y. and Wiens, D., *J. Geophys. Res.*, 1997, **102**, 27439–27451.
24. Parson, L. and Wright, I., *Tectonophysics*, 1996, **263**, 1–22.
25. Faul, U., Toomey, D. and Waff, H., *Geophys. Res. Lett.*, 1994, **21**, 29–32.
26. Zhao, D., Ochi, F. and Hasegawa, A., *J. Geophys. Res.*, 2000, **105**, 13579–13594.
27. Zhao, D., Kanamori, H., Negishi, H. and Wiens, D., *Science*, 1996, **274**, 1891–1894.
28. Zhao, D. and Negishi, H., *J. Geophys. Res.*, 1998, **103**, 9967–9986.
29. Zhao, D. and Mizuno, T., *Geophys. Res. Lett.*, 1999, **26**, 3213–3216.
30. Ishida, M., *J. Geophys. Res.*, 1992, **97**, 489–513.
31. Tsuboi, C., *J. Phys. Earth*, 1956, **4**, 63–66.
32. Kanamori, H. and Anderson, D., *Bull. Seismol. Soc. Am.*, 1975, **65**, 1073–1095.
33. Inoue, H., Fukao, S., Tanabe, K. and Ogata, Y., *Phys. Earth Planet. Inter.*, 1990, **59**, 294–328.
34. Bijwaard, H., Spakman, W. and Engdahl, E., *J. Geophys. Res.*, 1998, **103**, 30055–30078.
35. Flanagan, M. and Shearer, P., *J. Geophys. Res.*, 1998, **103**, 2673–2692.

ACKNOWLEDGEMENT. We thank Dr Kusala Rajendran for useful discussions and suggestions.